Planetary backup bearings for high speed applications and service life estimation methodology

Lukas QUURCK*, Daniel FRANZ*, Benedikt SCHUESSLER* and Stephan RINDERKNECHT*

* Institute for Mechatronic Systems in Mechanical Engineering (IMS), Technische Universität Darmstadt

Otto-Berndt-Straße 2, 64287 Darmstadt, Germany

E-mail: quurck@ims.tu-darmstadt.de

Abstract

Backup bearings (BB) limit the translational movement of rotors during malfunction, overload or power loss in the active magnetic bearings (AMB) in order to enable safe spin down and reduce secondary damage. Especially for high speed applications like flywheels with high rotor inertia, the requirements towards the load capacity and service life of the BB is comparably high. For a special type of flywheel with exceptionally high speeds in the BB interface, a planetary BB system is presented. The planetary BB consists of multiple bearing units placed circumferentially around the stator. Its elastic properties are described as well as a contact damping model. For cost efficient BB investigation, a scaled test rig is introduced and a parametric study of different delevitation simulations is done. Several quantification methods to evaluate severity, bearing loads and lifetime utilization during rotor delevitations are presented and applied to the simulations. Using a dry friction model a service life estimation of MoS_2 ball bearing lubrication is made. The applicability of the planetary BB to vertical high speed rotors is confirmed by the simulation data and bearing element selection is affirmed. The results of the quantification methodologies show specific correlation to initial conditions and parameters like unbalance and in particular friction coefficient. Further the influence of the rotor weight and size to the bearing loads is investigated.

Key words : Backup bearing, Flywheel, Kinetic energy storage, Lifetime, Service life

1. Introduction

Flywheels for energy storage applications commonly use contact free magnetic bearings in order to reduce losses and maintenance. As most magnetically levitated rotors, flywheels need backup bearings (BB) for safety and availability. The task of the BB system is to limit the rotor translational movement during malfunction, overload or power loss in the active magnetic bearing (AMB) in order to enable safe spin down and reduce secondary damage. Advanced flywheels combine high inertia with high rotational speed to achieve high energy density. This increases the requirements for the BB system in terms of requested service life which can be several minutes for a single spin down.

In case of hollow cylinder shaped, hubless, outer rotor type (ORT) flywheel the rotor inertia and the surface speeds are comparably high. At the inner diameter, more than 200 m/s occur, which is faster than most conventional shaft rotors. Special challenges of ORT BB are described by Quurck, et al. (2014) as well as the planetary BB system which was chosen for ORT flywheels. The planetary design was derived by the approach of Chen et al. (1997) and was similarly presented by Jansen et al. (2014) in a specific flywheel BB application. The use of multiple comparably small bearing units in each BB plain in circumferentially arrangement uncouples the rotor diameter from the needed bearing size and promises better high speed capability while acting as a resistance for destructive whirl motions.

2. Research objectives and approaches

The main objective of the BB research at the IMS is to find a suitable BB system for high speed ORT flywheels like the 1.5 kWh prototype “ETA290” with 290 mm inner rotor diameter and a top speed of 14100 rpm. The flywheel is used in an industrial application for load smoothing and peak shaving. Larger systems with more than 2.4 kWh are currently under implementation. Figure 1 shows a photo of the ETA290 flywheel system installed in the utility compartment of the ETA Factory which is a model factory built within a research project between 2013 and 2017.

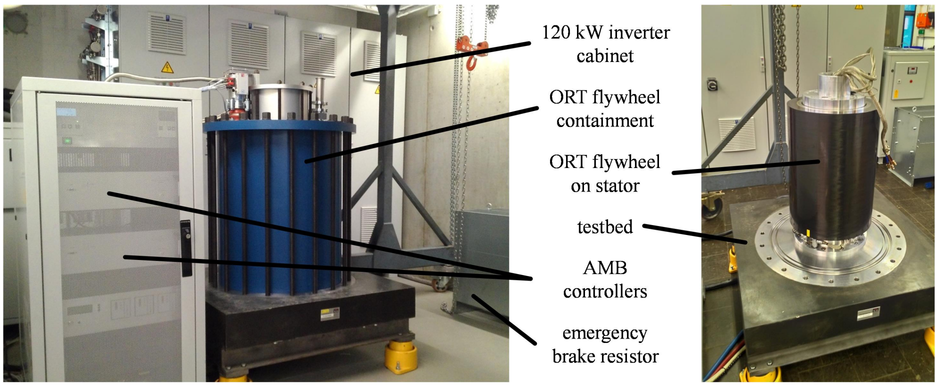

Fig. 1 Photography of the ETA290 flywheel in an industrial application (left), flywheel mounted on stator without containment (right)

Furthermore, the investigation of service lifetime and failure modes associated to bearing components is targeted. Service lifetime denotes the number of endurable rotor delevitations from a distinct dropping speed or rather how long the bearing can withstand without bearing failure or consecutive component damage during drop downs. To approach a robust and durable BB system for an ORT flywheel, the dynamic behavior of the rotor-stator interaction needs to be investigated. For this purpose, simulations are made in the state space simulation environment ANEAS (Analysis of Nonlinear Active Magnetic Bearing Systems) (Orth and Nordmann, 2002), (Orth, 2007).

As every model is a simplification and contains assumptions as well as uncertain parameters, experimental testing for verification needs to be done. Because full scale experiments of the planetary BB system with flywheels are expensive and bear uncalculatable hazards to machines and environment, for this paper a substitute rotor and stator as well as its planetary BB is used for simulation and later experiments. The simulation data is processed by different evaluation methods which are compared to each other. The comparison between simulation and experiments will later be used for parameter identification and improvement of simulation results in order to reduce further experimental testing needs.

3. Test rig design

The function of the test rig is to mimic the dynamics of the ORT flywheel during rotor delevitation events (RDE), although the rotor is a conventional shaft rotor. Design criteria were comparable high bending eigenfrequencies as well as a ratio of polar and axial moment of inertia I_p/I_a which is near to the ORT flywheel. The ratio I_p/I_a describes the gyroscopic properties of the rotor. For a homogenous sphere with high gyroscopic characteristics it is equal to one and for long thin cylinders with low gyroscopic eigenbehavior it is near to zero. As a specialty of the ORT flywheel the maximum surface speed of the BB should be reproduced by the test rig rotor. Furthermore, the rotor should be built from high strength steel with bigger mechanical and thermal robustness than the ORT flywheel made of fiber-reinforced plastic (FRP). After an iterative process, a modular and symmetric rotor design with exchangeable primary BB disc plains was found to fit the requirements best. Some properties of the original flywheel rotor “ETA290” and the test rig are given in Table 1. Fig. 2 shows a 3D model of the test rig rotor design and Fig. 3 shows a BB plain of the test rig consisting of the stator and 6 BB units. The test rig is planned to be set up in early 2017 and multiple RDEs in different BB configurations are intended.

The test rig rotor is magnetically suspended by two radial AMBs and driven by a permanent magnet (PM) synchronous machine. The axial levitation is done by an AMB sitting in between the two primary BB discs. The axial AMB is intended to levitate the rotor during RDEs in order to avoid axial contact. This is important because the ORT flywheels are axial levitated by PM bearings which are comparatively reliable and robust against external influence.

Table 1 Comparison of the flywheel and test rig

feature	unit	ORT “ETA290”	test rig rotor
1st bending eigenfrequency	Hz	1152	1469
2nd bending eigenfrequency	Hz	1219	1851
inertia ratio I_p/I_a	-	0.65	0.58
rotor mass	kg	149.4	18.1
max rotation speed	rpm	14100	21000
BB diameter	m	0.29	0.21
max BB surface speed	m/s	243	230

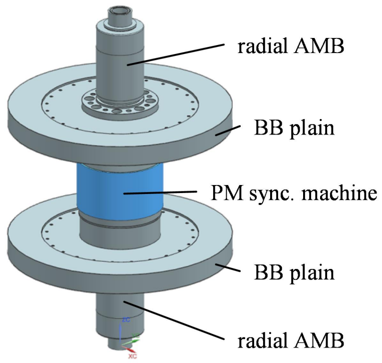

Fig. 2 3D Model of test rig rotor

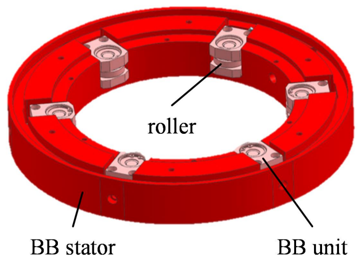

Fig. 3 Test rig planetary BB with six BB units with each two ball bearings and one roller

4. General modeling approach

Within ANEAS, discrete models of rotor and stator are transformed to state space model. In order to reduce the computational effort, the eigenmodes of the uncoupled rotor and stator are truncated, which have small Hankel singular values and consequently do not contribute much to the global dynamic behavior of the system. Coupling between rotor and stator can be performed by the AMB and its controller dynamics, as well as through different types of BBs, like plain bearings and several types of rolling element bearings. The set of possible BB types was extended for this work by the planetary BB design. Within the simulation all rolling element bearings use extra rotational degrees of freedom (DOF), and are fixed to translational DOF of the stator. The rotor-stator coupling in this work results from the mechanical contact force and a negative radially symmetric stiffness of the PM synchronous machine. AMB forces are set to zero in order to represent a complete power loss. Due to the vertical orientation of the flywheel and test rig rotor, gravitation is neglected.

Both, rotor and stator are modelled with Timoshenko beam finite elements with 4 DOFs per node. The discretization of 32 elements at the rotor and 16 elements at the stator showed good agreement with a detailed 3D numeric modal analysis. Internal structural damping is considered by assuming 1 % modal damping. Fig. 4 shows the geometry and discretization of the used rotor and stator models.

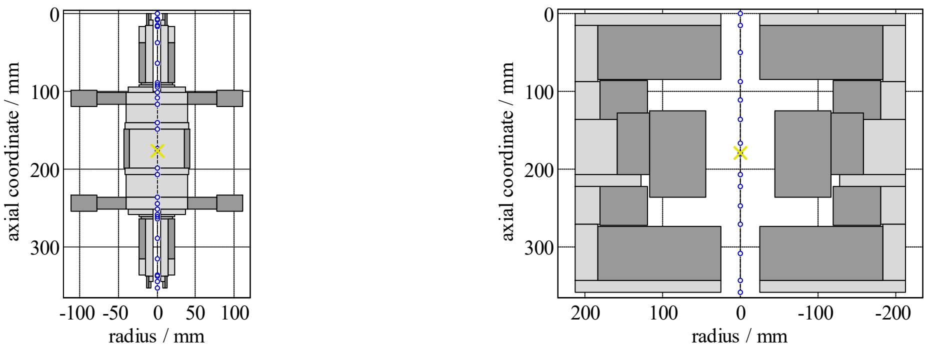

Fig. 4 Model of rotor (left) and stator (right) of BB test rig. Blue dots represent nodes, yellow cross the center of gravity.

The contact forces normally increase disproportional to the deflection, because they are generated by hertzian contact elasticities of bearing components. To take this into account, nonlinear analytic calculation or experimentally generated force-deflection curves need to be regarded as well as a realistic contact damping model. The basic contact model is illustrated in Fig. 5 and explained in the following section. The complex multiple serial and parallel elastic model was simplified to a single DOF substitute elasticity with a suitable damping model, as illustrated in Fig 7.

4.1. Static elastic compliance of BB components

The nonlinear stiffness of the BB components determines the radial forces applied between rotor and stator and therefore their dynamics during RDE. For rolling element bearings the elastic compliance can be determined analytically with good accordance to measurements. Gargiulo (1980) gives a simplified analytic formula given in Eq. (1), to calculate the static, radial force F_{static} for given bearing inner ring deflection δ of standard bearings using only the number of rolling elements Z, the rolling element diameter D_m and the contact angle β.

$$F_{static} = 2.192 \cdot 10^{10} \cdot Z\sqrt{D_m \cdot \delta^3 \cdot \cos^5 \beta} \tag{1}$$

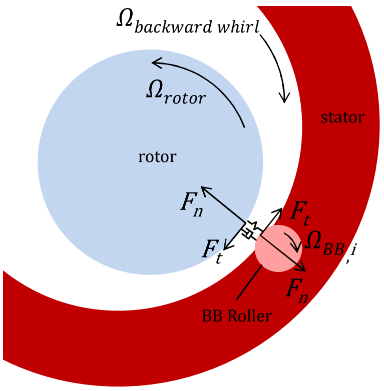

Fig. 5 Contact model used for simulation

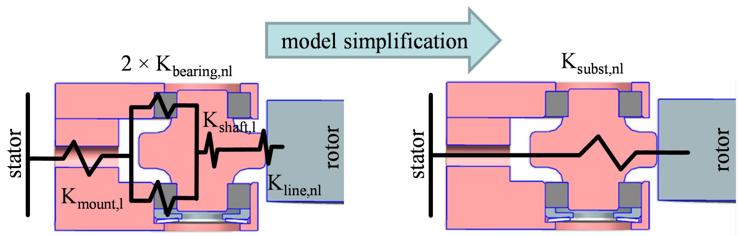

Fig. 6 Illustration of the discrete model of the elasticities of a BB unit. Left: parallel and serial elasticities. Right: simplified, nonlinear model used in simulation

In Fig. 8 a force deflection curve is shown for two parallel standard deep groove bearings of type 6001, with 8 balls each, marked with the black pointed line. In the case of the planetary BB design multiple serial and parallel elasticities of a single BB unit have to be considered for an accurate calculation. Fig. 7 shows a vertical cross section of a BB unit with an overlaid model of the discrete elasticities k_i. The index nl labels nonlinear and l linear characteristics. In order to reduce the complex elasticity to a single force deflection relation, an experiment was carried out in which the real elasticity of all present components in a realistic setup is represented. During the quasi-static experiment, the total deflection between a hardened steel plate and a bearing mount was recorded along with the applied force. The measured force deflection curve in Fig. 8 is used further to determine the static contact force F_{static} by the calculated deflection in the simulation.

4.2 Contact damping

In case of nonlinear and impact like contact situations a linear damping approach like $F_{damp} = d\dot{\delta}$ does not show a good accordance to real physical experiments. Especially negative contact forces, due to negative deflection velocities, shown in Fig. 7 as dashed blue line, disagree with mechanical reality. Another unrealistic feature of the linear damping approach is the discontinuous force at the beginning of the contact, where it is expected to be zero.

Microscopic plastic deformation and friction induced dissipative processes in the contact patches of impacting bodies can be macroscopically described by the coefficient of restitution. Hunt and Crossley (1975) created a modeling approach for impacting bodies which can describe vibro impacts with high accordance to experiments. The resulting dynamic contact force F_{dyn} can be written as in Eq. (2).

$$F_{dyn}(\delta, \dot{\delta}) = F_{static}(1 + 1.5\,\alpha\,\dot{\delta}) \tag{2}$$

The basic idea of this approach is to expand the static elastic contact force F_{static} using the damping coefficient α multiplied with deflection velocity. An energy dissipating hysteresis loop can be displayed when contact force is plotted over deflection in Fig. 7 in red solid line. The area enclosed by the loop quantifies the dissipation during contact. The approach of Hunt and Crossley delivers speed dependent, continuous, non-zero crossing contact forces and can be applied to different static elastic characteristics. In Fig. 7 exemplary calculation based on a static force deflection curve of Gargiulo is displayed and compared to linear damping and the Hunt & Crossley Model with an arbitrarily value of α = 3 s/m. Fig. 8 repeats the same with the static measured force-deflection curve of the BB unit mentioned in the section above. This curve combined with the Hunt and Crossley contact damping approach with a value of α = 5 s/m, derived from bouncing tests was chosen for further simulation.

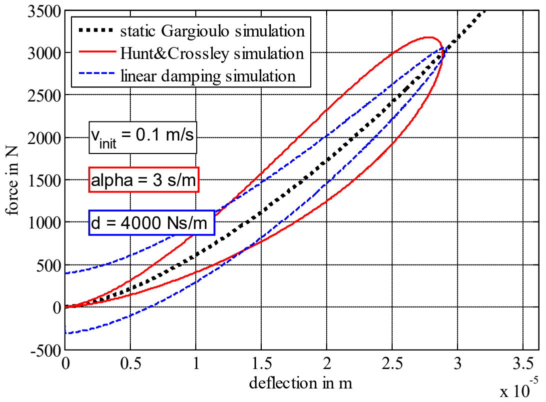

Fig. 7 Calculated static and dynamic force deflection curves of two parallel 6001 steel ball bearings

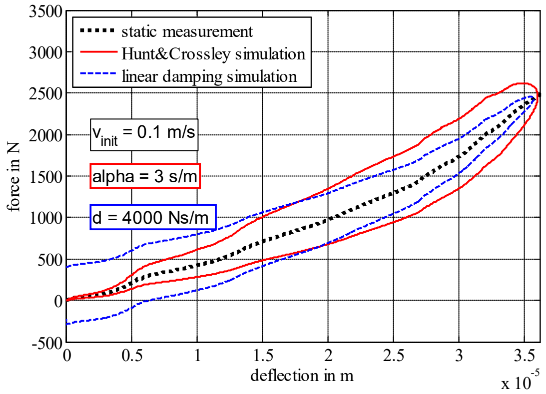

Fig. 8 Measured static force deflection curve of a bearing unit and different damping models

4.3 Friction

The relative velocity between rotor and BB surfaces causes tangential friction forces during contact, which accelerate the rotational states of the BB units and decelerates the rotor's rotation. Simultaneously the friction forces affect the rotor's translational states. Typically the tangentially acting friction force causes backward whirl motions. Because of its dry character the assumption of Coulomb friction is an appropriate approach. In Eq. (3) a steady approximation of Coulombs friction law is given. It calculates the direction dependent friction force $\boldsymbol{F_{fric}}$ using the friction factor μ, the relative surface speed Δv and the normal force which was calculated before as the dynamic contact Force $\boldsymbol{F_{dyn}}$.

$$F_{fric} = \mu \cdot F_{dyn} \cdot \left(\frac{2}{\pi}\arctan(100 \cdot \Delta v)\right) \tag{3}$$

With viscous bearing lubrication the friction can be approximated by classical drag moment models described in bearing catalogs such as Schaeffler (2008). Eq. (4) gives the drag moment of one single bearing. It consists of a speed dependent part M_0 and a load dependent part M_1. This model was used in the presented simulation model.

$$M_{drag,BB} = M_0 + M_1 \tag{4}$$

The values of M_0 and M_1 have to be calculated from manufacturer data and with the knowledge of the temperature dependent kinematic viscosity of the lubricant. The value was assumed to be $5\ \mathrm{mm^2/s}$ for simulation.

5. Planetary BB orbit

The planetary BB system has a noncircular clearance orbit which is defined by the enclosed area of the herpolhodes of the rotor touching the BB rollers. Fig. 9 illustrates the clearance orbit of the rotor in a BB system with only 3 rollers.

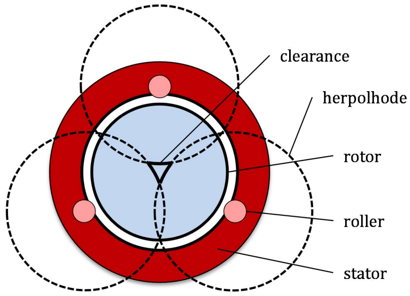

Fig. 9 Schematic illustration of the clearance build with three BB

The curvature of each section of the clearance orbit is defined by the sum of rotor and stator radius and represents the herpolhodes of the rotor touching the BB rollers. For simulation the curvature of the herpolhodes was neglected and simplified to straight lines. Connected to each other these straights form a polygon shaped BB orbit. The noncircular BB orbit leads to altered delevitation behavior compared to a circular orbit. The continuous contact during a whirl is prevented because every change of polygon section results in a new impact, leading to bouncing rotor reaction. Former works from Helfert (2008) showed a whirl suppressing effect of deviation roller elements inserted in a conventional circular BB orbit. First tests confirm the jumping character of the rotor trajectory inside a planetary BB. The occurring backward whirl motion remained at low frequencies what can be explained by the soft and highly impact damped contacts of the BB units, compared to conventional BB bearings where the forces against whirling are dominated by rolling resistance rotor inside the inner bearing ring. Simulation results substantiate this assumption. However, high speed testing has to be performed to definitely verify the general whirl resistance of a planetary BB system.

6. Evaluation of simulation results

Main interest of the simulation of RDE is the global dynamic behavior and the contact forces which may damage the rotor or the BB components. Therefore, simulation results contain all translational states of the rotor and stator, their translational and rotational speed, the tangential and radial forces of each BB unit and their rotational speed. Generally, RDEs deliver large amounts of data which have to be processed to classify or preferably quantify the severity of the RDE, the occurring wear or the expected remaining service life of a bearing. The identification of harming loads or excessive rotor movements therefore is important for automated evaluation of experimental or simulation data. Several methodologies using different information can be used and are described in the following sections.

6.1 Position data based evaluation

One possibility is to evaluate the rotor's translational states in bearing or sensor plain. Janse van Rensburg (2015) proposes to calculate the length of the rotor trajectory normalized by the nominal air gap of the BB during a RDE. The dimensionless value is called D_{val}. This analysis of the position data can differentiate between different whirl movements and less harming behavior with shorter trajectories and therefore classify the severity of an RDE. Experimental testing with non-lubricated standard bearing showed correlation between D_{val} and the occurring bearing wear during and after multiple consecutive RDEs. Janse van Rensburg explains this correlation with the growing inner friction inside the bearing. Debris from surface erosion due to spot welding between steel balls and races, or wear of the steel cages can be assumed as reason for the observed bearing degradation. The growing bearing friction at some point results in harsher RDE with high whirl probability and high D_{val} numbers. The negative influence of worn or polluted bearing were also observed by Helfert (2008) after contaminating steel BBs with tar and chalk, which heightens the inner friction and rises the whirl probability from 8% to 30%. Helfert classified the rotor movement by analyzing the rotor position in the BB plain and by assessing the occurring whirl frequencies. The occurrence and the height of whirl frequencies are measures for severity assessment, but still need experimental comparison data to evaluate wear and remaining bearing life.

6.2 Bearing load based evaluation

One other possibility is to use the loads and rotational speeds of the BB. It is evident that these values can deliver more information about bearing wear than using only rotor states. As a downside of this approach the interpretation of these values may be more difficult, and experimental investigation with load cells and BB speed recording still needs to be done, which is often too expensive to be implemented in serial production. Nevertheless the necessary data acquisition can deliver important information for simulation reconciliation and parameter adjustment and is therefore useful for test rig settings.

By observing the transient force curves of BBs, the severity of RDEs and the utilization of the bearing element load capacity can be assessed. A physically motivated end of life criterion for rolling element is the comparison of the maximum force peak to the static load rating C_0 of the bearing. Exceeding this rating causes plastic deformation of bearing components and immediate loss of functionality by immense rise of inner friction.

The lifetime calculation of rolling element bearings following ISO 281 (2007) is supposed to calculate the number of revolutions at a defined load and rotational speed that a bearing can withstand at a certain failure probability. As failure mechanism fatigue of steel interfaces is postulated. Fatigue is caused by the swelling Hertzian contact stress of the rolling elements overrunning the raceway repeatedly during bearing rotation. For a desired failure probability of 10 % the number of revolutions multiplied by 10^6 is given by Eq. (5)

$$L_{10} = \left(\frac{C}{P_{eq}}\right)^p \tag{5}$$

The dynamic load rating of the bearing is C, while P_{eq} stands for the applied equivalent load and the exponent p is a bearing type dependent constant. For ball bearings it is equal to 3. The dynamic load rating can be delivered by the manufactures and is based on empirical data. For BBs of flywheels with viscous lubrication a similar lifetime prediction has been developed by Sun (2006).

Applied to the short, but very dynamic BB loads, the validity of the probabilistic fatigue model of the ISO 281 may be mistrusted in its original meaning. Especially the absence of thermal influences and realistic adjustment factors concerning varying lubrication and contamination will lead to deviations from experiments. Nevertheless, the calculated and measured lifetime L_{10} is expected to correlate to simulated or measured bearing loads. If the general assumption that a higher bearing load will lead to a lower lifetime comes true, low L_{10} values indicate RDEs with higher severity than RDEs with higher L_{10} values. Like D_{val} this offers the opportunity to compare different RDEs and gain more certainty about bearing selection and their service lifetime.

6.3 Dry lubricant wear

In vacuum application bearings are often lubricated with dry lubricants like molybdenum disulfide (MoS_2), silver or other thin film coatings. Dry lubricated bearings offer nearly speed and temperature independent low friction operation and do not suffer from evaporation like liquid lubricants. These properties make dry lubrications predestinated for vacuum operated BBs of flywheels. As a downside of dry lubricants, their service life is determined by the mechanical wear induced by slipping inside the hertzian contact patches. Further information about applying, handling, properties and wear of dry lubrication is given in the space tribology handbook of the ESTL (1998).

To calculate the service life of dry lubricated bearings, the methodology of Birkhofer and Kümmerle (2012) can be applied. The theory is based on the proportionality between dry frictional energy and wear of the bearing lubricant and the resulting service life which is inversely proportional to the frictional energy, written in Eq. (5).

$$frictional\ energy \sim wear \sim \frac{1}{service\ life} \tag{5}$$

The end of life criterion is exhaustion of the dry lubricant at the place inside the bearing of highest frictional energy generation. Once the lubricant is worn, the friction inside the bearing rises significantly and overheating as well as excessive surface erosion is likely to occur. Immediate bearing failure has to be expected. To calculate the frictional energy inside the bearing, the local loads have to be known from which the hertzian contact stresses $p(x, y)$ and the slip $s(x, y)$ between balls and races can be calculated. Using the elliptic contact patch area A, the friction coefficient

μ and the length of the contact patch b in rolling direction, the frictional energy E_{fric} per overrun can be calculated by Eq. (6) for a certain position in the bearing.

$$E_{fric} = 2 \cdot \mu \cdot b \int_A p(x, y) \cdot s(x, y) dx\, dy \tag{6}$$

In order to calculate the local frictional energy during transient loading, every overrun has to be summed. The cumulative frictional energy inside a bearing during the transient load is the sum of all local frictional energies.

Figure 10 shows results of a full speed RDE simulation of the test rig rotor in a planetary BB. The normal contact force is plotted together with the rotational speed of one of the BB units in the upper plain. Below the calculated cumulative frictional energy is displayed. The bearing unit is accelerated intensively between 0.6 and 0.8 seconds when the rotor touches the BB unit. This normal force leads tangential dry friction force which accelerates the BB unit. During this phase the cumulated frictional energy inside the bearing rises with every contact. When no load is applied on the BB unit the frictional energy remains unchanged because no axial preload is applied and friction between balls is neglected. Extra load from the centrifugal forces of the ceramic balls are included but have very little influence to the overall frictional energy generated inside the bearing.

To calculate the service life of the dry lubricant, its volume at the highest loaded area has to be known as well as the specific wear rate of the coating. Latter depends on the coating process parameters, the vacuum quality during usage and the presence of H_2O vapor, (Roberts, 1987). It can be derived from experiments like pin on disc tests. When lubricant wear rates are known it is possible to calculate how much of the lubricant is worn during the simulation. Birkhofer and Kümmerle (2012 p. 207) investigated wear rates of 2.29e-6 mm³/mJ for PVD sputtered MoS_2 lubricant coats at 250°C. For this work the calculation was done with a higher wear rate of 1e-5 mm³/mJ in order not to overestimate the lubricant lifetime. A remaining service life in terms of remaining allowable RDEs could be given. In the given simulation it was calculated that the bearings MoS_2 lubrication can withstand 3.4 full speed drops. This result has to be seen as first estimation. Experimental investigation needs to be done in order to proof wear rates which highly depends on the coating process and the accessible wear volume inside the bearing geometry. However, as comparative value for severity of different RDEs the value of frictional energy can be used.

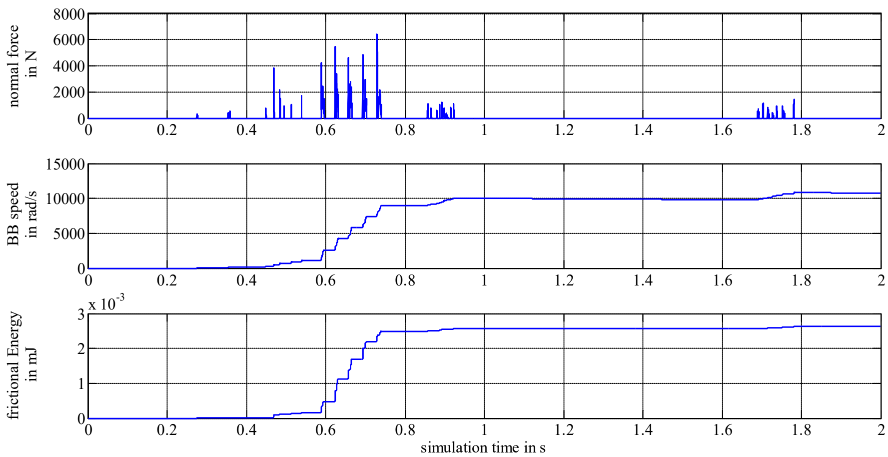

Fig. 10 Simulation results of a single BB unit of the test rig. The frictional energy was calculated by a dry friction model for a MoS_2 coated hybrid ball bearing.

7. Simulation

In order to analyze general influence and sensitivities of RDEs towards parameters and system properties two investigations are presented. First is a parametric study using the rotor and stator model described in Section 4 and the planetary BB design mentioned in Section 5. The second investigation concerns the influence of the scale of the rotor in order to proof the validity of the results of the first investigation towards heavier flywheels.

7.1 Parametric study

A parametric study was carried out with 35 simulations, each with a simulated time of 10 s. The simulations were grouped by five parameter sets, each with a single changed parameter. In each parameter set the starting rotational speed of the rotor n_0 was varied in seven steps from 4000 to 20000 rpm. In all simulations the starting position was 50% of the radial air gap of 0.42 mm measured from the center of the BB. The rotor was released with a defined starting velocity v_0 in backward whirl direction. In order to evaluate the sensitivity towards initial translational starting velocity v_0, friction factor μ and total unbalance U, one of these parameters were changed in each parameter set for all seven associated simulations. Table 2 contains the used parameters. In all simulations, no active braking is applied by the electric machine.

Table 1 Parameters of 5 different parameter sets. With every parameter set 7 RDEs with different rotational starting speed were carried out. Only the changed parameter is noted. Missing entries indicate that the value of the reference set was used.

		parameter set name				
parameter name		reference	$2U$	$0.5U$	$10v_0$	μ=0.1
starting velocity v_0	m/s	0.01			0.1	
total unbalance U	kg m	5.62×10-5	1.12×10-4	2.81×10-5		
friction coefficient μ	-	0.15				0.1

For illustration purposes, simulation data of the reference parameter set at a starting rotational speed of 20000 rpm is presented. The rotor position in the upper BB is displayed in Fig. 11. Figure 12 shows the translational velocity plotted over time. In Fig. 13 the corresponding contact normal force on the rotor is displayed. The position plot shows that most of the time the rotor is near or contacting the BB, while the center of the BB orbit is passed comparably rarely. During contact the rotor position is displayed outside the polygon. Induced by the tangential friction force the translational rotor movement is a backward whirl, plotted clockwise. The normal contact force shows distinct phases where no contact occurs, indicating that the rotor does not continuously roll in the BB. The contact force also indicates two phases where high force peaks occur. During these phases the rotor performs its highest translational speeds of around 0.2 m/s and the BB units are accelerated to the synchronous speed, while the rotor loses 7 % of its rotational speed in 1 s. After this friction intensive phase, the translational rotor movement slows down and normal forces decrease. After synchronization the rotational speed of the BB units and the rotor decreases by 3 % in around 9 s due to the bearing friction. This global behavior can be found in all 35 simulations. Differences were basically registered in the height of forces and velocities as well as the time when synchronization takes place. No synchronization after 3 s occurred, indicating that the first 3 s are most crucial for the BB loads.

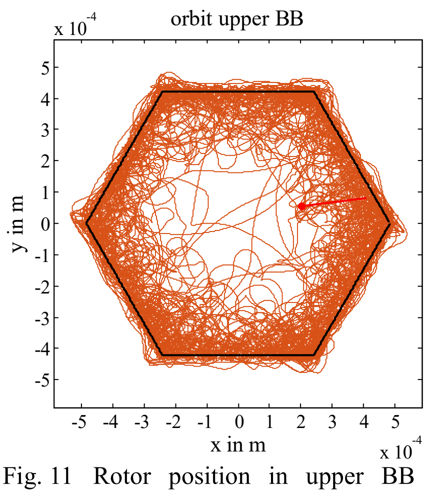

Fig. 11 Rotor position in upper BB plain during a 10 s RDE

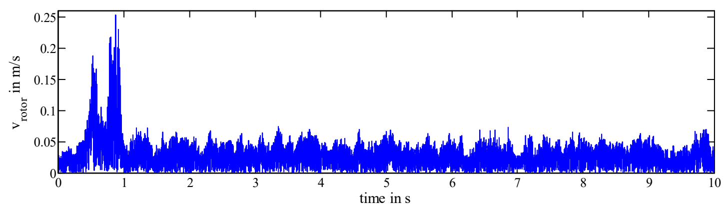

Fig. 12 Translational rotor velocity in upper BB plain

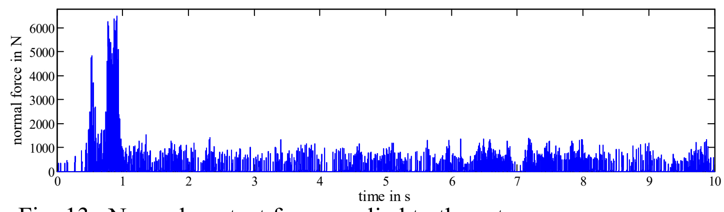

Fig. 13 Normal contact force applied to the rotor

7.2. Scalability

Within the design processes of conventional bearings the weight of the machine is often an important design parameter and corresponds to the necessary load rating and size of the bearing. Within vertically oriented rotors the influence of the gravity to the bearing loads is less important and can often be neglected. However, the mass of the rotor has major influence on its eigenbehavior. The influence of mass to highly nonlinear dynamic system like rotor-BB-interactions cannot be predicted and has to be investigated. This investigation is of special interest for the evaluation of later experiments in order to transfer the results of the light weight test rig rotor to much heavier flywheels. In order to observe the influence of the rotor scale a second rotor model was created for simulation with enlarged lengths and diameters while the dynamic properties like elastic eigenfrequencies of the rotor where kept nearly the same. The mass of the scaled rotor model is 159 kg, which is 8.8 times the mass of the test rig rotor model and close to the ORT flywheel. The stator size was scaled in the same way. The bearing units were kept the same size and defined by the same elastic and dynamic properties. With this scaled model seven delevitation simulations with different starting speeds were carried out using the same initial conditions and parameters like the reference set described in Section 8.1.

8 Results

The results of the parametric study and the scaled rotor model simulations are presented in the following sections. The methodologies described in Section 6.1 and 6.2 are applied to the simulations and interpreted. The evaluation of the dry lubricant wear described in 6.3 is not presented because the lack of coating data, which could not be provided by manufacturers.

8.1 Parametric study results

The evaluation results of the first 35 simulations with the test rig model are plotted over the initial rotational speed in Fig. 14 to 17. First, the maximum force F_{max} was assessed to evaluate plastic deformation. As can be seen in Fig. 14 in almost every simulation set, F_{max} rises with an increase of rotor speed. In parameter set 2U the highest loads occur while 0.5U tend to the lowest loads. An increased staring velocity does not significantly increase F_{max}. In Fig. 15 the total revolutions of a BB unit during a simulation divided by the L_{10} lifetime is displayed. The analysis was done for the BB unit with highest ratio in order to emphasize the most critical unit. This ratio can be interpreted as lifetime utilization value. The higher the calculated value is, the more likely a bearing failure is. In other words, it can be assumed that the higher a value is, the more the bearing is worn during the RDE. Initial translational speed v_0 does not have a significant influence on the results. A detailed analysis shows that after few impacts, the translational velocity develops independently from the initial contact. Same counts for the influence of the unbalance. Although the height of the unbalance seems to affect contact forces, the influence is comparatively low. The contact friction factor μ has a very high influence. In the low friction parameter set μ=0.1, the maximum contact force is reduced by roughly 50 % to the averaged values of the other simulations. Also the lifetime utilization value shows significantly lower values.

Of particular interest is how the D_{val} values correlate with the L_{10} values. Fig. 16 and Fig. 17 show both values for all simulations. D_{val} is very sensitive against different parameters. Especially the height of the unbalance has a strong influence on the results. With rising initial rotational speed D_{val} tends to higher values, indicating higher rotor movements and therefore dynamic loads. The correlation between D_{val} and the unbalance can be explained through the natural circular movement of the rotor caused by the unbalance force. In the interpretation of D_{val} special attention has to be given to the unbalance. A changed unbalance can be cause and effect of a RDE at the same time, what has to be regarded when analyzing changing D_{val} after consecutive RDEs. Examining L_{10} values, the correlation with starting speed is more significant compared to unbalance and v_0. Interesting results can be observed by the comparison of the low friction parameter set. While D_{val} indicates higher rotor movement, which would be interpreted as higher bearing wear, the L_{10} values indicate lower bearing loads and longer lifetime. This coherence needs to be investigated further and experimental testing will deliver more insight to the actual correlations.

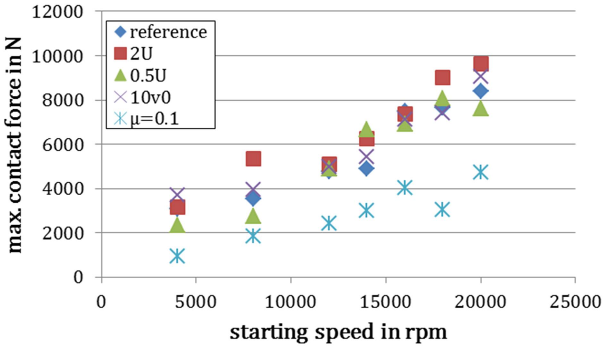

Fig. 14 Maximum contact force peak during simulations

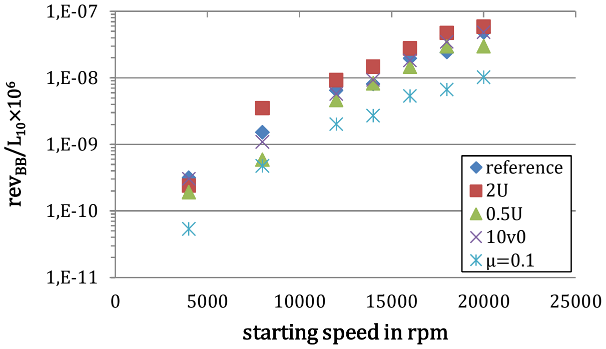

Fig. 15 Total revolutions of the most critical BB unit divided by calculated L_{10} lifetime

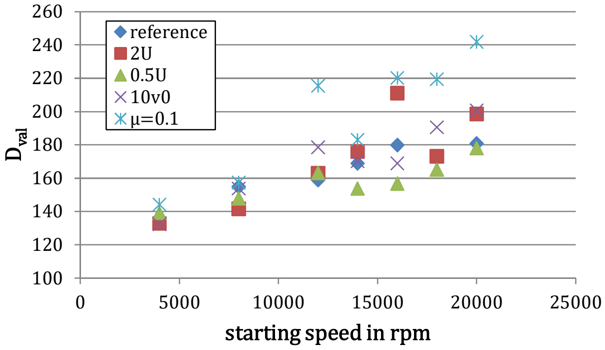

Fig. 16 D_{val} after 10 s simulations

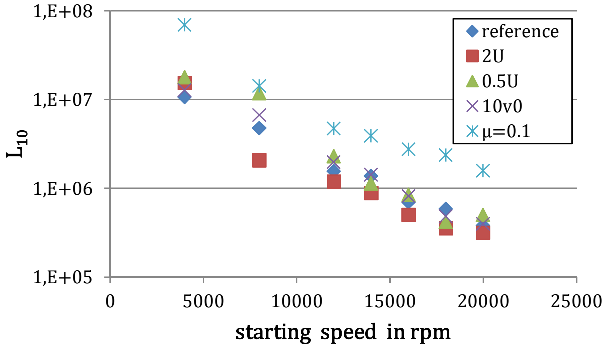

Fig. 17 L_{10} value after 10 s simulations

8.2 Scalability results

During all 10 s simulations with the scaled rotor and stator model the global behavior of the rotor is comparable to the simulation with the test rig model. Differences can be found in the heights of the translational speeds and the contact forces, what can be seen in the following assessments.

In Fig. 18 and 19 the maximum contact force and the lifetime utilization values of the 18 kg test rig rotor and the 159 kg rotor model are compared to each other. The reference parameter set was used for these simulations. At low starting speeds the contact force does not significantly differ. Above 12000 rpm the maximum contact force of the scaled rotor is considerably lower than the light weight rotor and does not exceed 4950 N. The same can be seen in at the lifetime utilization factors. The calculations show that the bearing wear of the heavy rotor at high dropping speed is lower and longer lifetime can be predicted. Closer investigation of the position data reveals that the translational speed and calculated D_{val} of the 159 kg rotor is lower than of the 18 kg rotor. The higher mass seems to reduce the backward whirl frequency. As an explanation for this the lowered coupling eigenfrequencies between rotor and BB unit can be assumed.

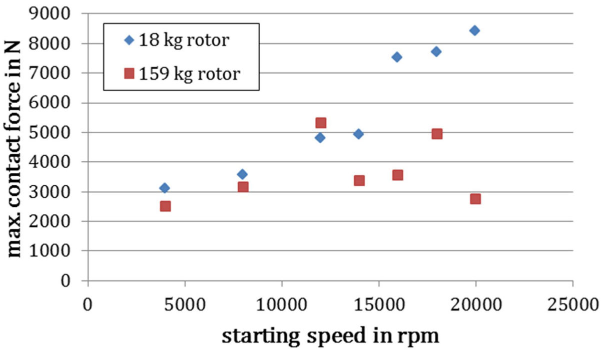

Fig. 18 Maximum contact force: The higher weight of the vertical Rotor lowers the maximum BB loads at high speeds

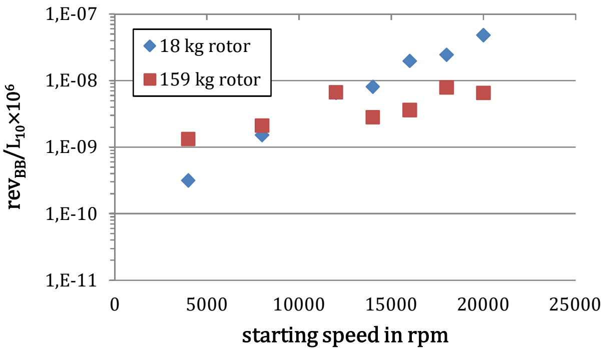

Fig. 19 Lifetime utilization: The lowered bearing loads lead to lower lifetime utilization values

As a result, it can be said that for vertical flywheel rotors, higher rotor weight does not necessarily increase the needed static or dynamic load capacity of the bearing. Potentially the bearing size can be reduced to gain more high speed compatibility, lower bearing inertia and lower bearing friction without losing lifetime. Due to simulation an alternative bearing selection can be recommended in order to improve BB performance.

9. Conclusion

This work shows different ways to quantify the severity of RDEs using force, rotational BB speed and position data. In the design phase especially the force dependent quantification data helps to assess dynamic simulations and can give information about the selection and design of BB components. The used modeling and simulation environment of ANEAS can deliver the necessary simulation data for conventional and planetary BB design approaches. The simulation data of the planetary BB showed unproblematic RDE characteristics and acceptable bearing forces. An important result for the development of planetary BB is that the contact friction factor needs to be as low as possible, in order to lower translational rotor velocities and therefore bearing loads, even though the synchronization between BB and rotor takes more time.

The results of the parametric study show significant correlation to initial rotational speed and friction coefficient. The scale of the vertical rotor does not heighten bearing forces. For high initial rotational speeds, the bearing forces of the heavy rotor are even lower than the lighter.

During the design processes of a BB, the maximum contact force is a major design criterion. By calculating the L_{10} values of the simulation data, the comparison and classification of different delevitation events can be done. Correlation towards measured lifetimes still needs to be done. Because the lack of realistic adjustment factors for BB applications, especially in vacuum environments of flywheel direct lifetime prognosis from L_{10} calculation can only be used as a relative severity indicator.

10. Outlook

The showed test rig is going to be set up and put into operation. Then the simulation data needs to be verified. The experiments are going to deliver information about bearing wear, actual load capacity and service life of BB systems. To evaluate the frictional energy dissipation during RDEs, the test rig will be equipped with thermal sensors and speed sensors for the rotational BB unit states.

The planetary BB is going to be adapted to upcoming ORT flywheel prototypes and experimentally tested to assess the validity of the test rig results. The general goal is find a way to evaluate any BB system by simulation to determine an appropriate BB system. Being able to predict service life of the system without further expensive BB testing of the original rotor is the next goal.

References

Birkhofer H., Kümmerle, T., Dry lubricated rolling element bearings, Springer-Verlag, (2012) (in German)

Chen, H. Walton J., Heshmat H., Zero Clearance Auxiliary Bearings for Magnetic Bearing Systems, Paper No. 97-GT-112, ASME TURBO EXPO ‘97, Orlando, Florida, (1997)

Gariulo, E.P., A simple way to estimate bearing stiffness, Machine Design 52 (1980), pp. 107-110

Helfert, M., Rotor delevitaions in rolling element bearings – experimental investigation of rotor-backup bearing-contact, (in German), PhD. thesis, Darmstadt (2008)

Hunt, K., Crossley F., Coefficient of restitution interpreted as damping in vibroimpact, Transactions of the ASME, Journal of Applied Mechanics, pp. 440-445, (1975)

International Standardization Organization, ISO 281:2007 Rolling bearings - Dynamic load ratings and rating life (2007)

Janse van Rensburg, J.J. et al., Backup-Bearing lifetime prediction using quantified delevitation severity indicators, Proceedings of Workshop on Magnetic Bearing Technology 10, (2015)

Jansen R., Storozuk R., High speed, compliant, planetary flywheel touchdown bearing, WIPO Patent, WO2014/123507 A1, (2014)

Orth, M., Nordmann R., ANEAS a modeling tool for nonlinear analysis of active magnetic bearing systems, 2nd IFAC Conference on Mechatronic Systems, Berkley, USA, pp. 357-362, (2002)
Orth, M., Backup Bearing contact of magnetically suspended rotors (in German), Ph.D. thesis, Shaker Aachen, (2007)
Quurck, L., Schaede, H. Richter M. Rinderknecht S., High Speed Backup Bearings for Outer-Rotor-Type Flywheels – Proposed Test Rig Design, Proceedings of ISMB14, (2014)
Roberts, E.W., The Lubrication properties of magnetron sputtered MoS_2, ESTL Report, (1987)
Schaeffler, Wälzlager, manufacturer catalog, pp. 64 (2008) (in German)
Sun, G., Auxiliary Bearing Life Prediction Using Hertzian Contact Bearing Model, Journal of Vibration and Acoustics, Vol- 128, (2006)